

Long Noncoding RNA MIAT Regulates Hyperosmotic Stress-Induced Corneal Epithelial Cell Injury via Inhibiting the Caspase-1-Dependent Pyroptosis and Apoptosis in Dry Eye Disease

Jinjian Li^{1,*}, Kun Yang^{2,*}, Xinghui Pan¹, Hui Peng¹, Chenting Hou¹, Jie Xiao¹, Qing Wang¹

¹Ophthalmology, Affiliated Hospital of Qingdao University, Qingdao, 266500, People's Republic of China; ²Medical Research Center, Affiliated Hospital of Qingdao University, Qingdao, 266500, People's Republic of China

*These authors contributed equally to this work

Correspondence: Qing Wang, Ophthalmology, Affiliated Hospital of Qingdao University, 16 Jiangsu Road, Qingdao, 266500, People's Republic of China, Tel +86 17853290636, Fax +86 532 82911747, Email wangqing6836@sina.com

Purpose: The biological role and mechanism of long noncoding RNA (lncRNA) myocardial infarction-associated transcript (MIAT) in dry eye remain to be illustrated. Pyroptosis is a noticeable form of inflammatory activation, which is characteristic of gasdermin D (GSDMD)-driven cell death. The present study was designed to explore the role of MIAT in pyroptosis and apoptosis induced by hyperosmolarity stress (HS) in human corneal epithelial cells (HCECs).

Methods: HCECs were cultured in 70–120 mM hyperosmotic medium for 24 h to create a dry eye model in vitro. The level of the pyroptosis marker GSDMD was measured, and the cell inflammatory response was evaluated by detecting IL-1 β and IL-18 levels. Exogenous caspase-1 inhibitor Ac-YVAD-CHO was used. The pyroptosis in HCECs was examined by caspase-1 activity, immunofluorescent staining, and Western blotting. Flow cytometry was performed to test the apoptosis rate of HCECs. Cell migration and proliferation were detected. The expression of the lncRNA MIAT in HCECs was detected by quantitative real-time PCR. MIAT was knocked down by small interfering RNA (siRNA) transfection. The effects of caspase-1 inhibition on pyroptosis, apoptosis, migration, and proliferation were observed.

Results: HS promoted pyroptosis in HCECs by elevating caspase-1, GSDMD, and the active cleavage of GSDMD (N-terminal domain, N-GSDMD), and increased the release of IL-1 β , IL-18, LDH and the rate of apoptosis, with reduced cell migration. These changes were prevented by the inhibition of caspase-1. The expression of MIAT was significantly increased in HCECs exposed to a hyperosmotic medium. Silencing MIAT increased the expression of GSDMD, caspase-1, and inflammatory chemokines IL-1 β and IL-18, and promoted apoptosis while inhibiting migration and proliferation in HCECs.

Conclusion: The lncRNA MIAT is involved in HS-induced pyroptosis and apoptosis and the inflammatory response of HCECs and provides a new understanding of the pathogenesis of dry eye.

Keywords: myocardial infarction-associated transcript, dry eye, pyroptosis, apoptosis

Introduction

Dry eye is a multifactorial disease of the ocular surface, characterized by the loss of the homeostasis of tear film accompanied by symptoms of the ocular surface.¹ Hyperosmolarity-triggered inflammation and ocular surface damage are thought to play prominent roles.² Increased tear osmolarity activates multiple stress signaling pathways in the cornea epithelium and resident immune cells, triggering the secretion of many inflammatory biomarkers, such as IL-6, TNF- α , and MMP-9, which can be regulated by hydrocortisone.^{3,4} Some long noncoding RNAs (lncRNAs) have been observed to be elevated in human corneal epithelial cells (HCECs) induced by hyperosmolarity.⁵ Incidentally, differential lncRNA expression has been elucidated before and after hydrocortisone administration of bone

microvascular endothelial cells from the human femoral head, which emphasized that hydrocortisone can potentially modulate lncRNA.⁶

Long noncoding RNAs (lncRNAs) are a series of transcript RNAs larger than 200 nucleotides with limited or no protein-coding capacity.⁷ Recently, lncRNAs were shown to play a significant role in the pathogenesis of ophthalmological disorders such as glaucoma, corneal diseases, cataract, diabetic retinopathy, proliferative vitreoretinopathy, and ocular tumors.⁸ lncRNA myocardial infarction-associated transcript (MIAT) is associated with the regulation of vascular function, including corneal angiogenesis, retinal angiogenesis, and vascular leakage, and has also been identified as a regulator of retinal neurodegeneration in diabetes.⁹ In our former study, MIAT seemed to inhibit the expression of IL-1 β , TNF- α , and be suppressed by the NLRP3 inflammasome activation pathway.¹⁰

Pyroptosis is featured by caspase-1/11-induced gasdermin D (GSDMD)-driven cell lysis. Caspase-1 processes pro IL-1 β and IL-18 into their mature forms in the inflammasome pathway, and can also cleave the pore-forming protein GSDMD into its active form N-GSDMD, leading to the plasma membrane rupture and the release of intracellular contents, ultimately causing local or systemic inflammatory responses.^{11,12} Pyroptosis has been found to be involved in a variety of ocular diseases such as diabetic retinopathy,¹³ acute glaucomas,¹⁴ and *Aspergillus fumigatus* keratitis.¹⁵ Very recently, Chen et al showed that GSDMD-driven pyroptosis was involved in desiccating stress-induced dry eye mice.¹⁶ In addition to pyroptosis, caspase-1 also participated in apoptosis under the circumstances of inflammation.¹⁷

Here, we established an in vitro cell model of dry eye. MIAT was verified that existing a higher expression in the dry eye compared to the control. We then examined the roles of MIAT in HCECs pyroptosis, apoptosis, and then migration. Our data highlighted the novel role of MIAT in mediating pyroptosis and apoptosis via the caspase-1, with effects on HCEC migration in vitro.

Materials and Methods

Cell Culture and Treatment

Human corneal epithelial cells (HCECs), a human SV40 immortalized corneal epithelial cell line (CRL-11135, HCE-2; ATCC, Manassas, VA, USA), between passages 10 and 20, were cultured as previously described.¹⁸ The immortalized HCECs were then treated with a different osmolarity, ranging from 312 to 550 mOsm, which was achieved by adding 0, 70, 90, 100, 110, or 120 mM sodium chloride (NaCl) (Sigma-Aldrich, St. Louis, MO, USA), with or without an irreversible inhibitor of the caspase-1 Ac-YVAD-CHO (#A8954, ApexBio Technology, Houston, USA, 1–10 μ M) or dimethyl sulfoxide (DMSO), which were added after treated with NaCl for 24 h.

RNA Interference

The small interfering RNA (siRNAs) specifically against MIAT (GenePharma, Shanghai, China) were used to transiently knockdown target genes in HCEC with Lipofectamine 3000 (Invitrogen, Carlsbad, CA, USA) following the manufacturer's instructions. Transfection of siRNAs in vitro was performed 24 h prior to hyperosmolarity treatment at the optimal cell confluency of 60–70%, with resuspended siRNAs at a final concentration of 50 nM in wells. After 24 h exposure to iso- and hyperosmolarity, the cells were harvested and lysed in RIPA buffer for cellular protein extraction and TRIzol for total RNA extraction.

Cell Viability Assay

According to the manufacturer's protocol, we used Cell Counting Kit-8 (CCK-8) assay to detect the proliferation rate of cells. In brief, 100 μ L of HCECs (1×10^4) suspension were seeded into 96-well plates, treated for 24 h with different concentrations of the hypertonic medium, and incubated with 10 μ L CCK-8 (Dojindo, Kumamoto, Japan) for 2 h. A microplate reader (Bio-Rad, CA, USA) was utilized to estimate the absorbance at 450 nm. In addition, a CCK-8 assay was also employed to determine the viability of HCECs under different transfections after treatment with 90mM sodium chloride for 24 h. Three independent experiments were performed.

Quantitative Real-Time PCR (RT-qPCR)

Total RNA was extracted from HCECs by using the TRIzol reagent (TaKaRa Bio Inc., Otsu, Japan). After synthesizing with the PrimeScript RT Master Mix (TaKaRa Bio Inc., Otsu, Japan), cDNA was used for quantitative PCR (qPCR) using SYBR[®] Premix Ex Taq[™] (Perfect Real-Time) (TaKaRa Bio Inc., Otsu, Japan). The GAPDH gene served as an internal control, and the relative mRNA level in the untreated group was regarded as the calibrator. The primers used in this study were as follows:

hGAPDH F-CAACGTGTCAGTGGTGGACCTG and R-GTGTCGCTGTTGAAGTCAGAGGAG hMIAT F-CTCAGGAGTGCTTCGGAGGA and R-TTTCACAGAGCATCGGAGGC;

hGSDMD F-CCAGGTCCCAGCCTTGCTCTTG and R-CTCAGTCCGGTCCTTAGGATCCAGT; hcaspace-1 F-CAGCCAGATGGTAGAGCG and R-CCTGCCCACAGACATTCA;

hcaspace-3 F-GCTATTGTGAGGCGGTTGT and R-AGCAGGGCTCGCTAACTC;

hIL-1 β F-CCACAGACCTTCCAGGAGAATG and R-GTGCAGTTCAGTGATCGTACAGG;

hIL-18 F-GTCGCAGATGGCTCTTTGCT and R-TGCCAAAGTAATCTGATTCCAGGT;

The $2^{-\Delta\Delta C_t}$ method was applied to quantify the gene expression. Each sample was analyzed in triplicate.

Western Blotting Analysis

Cells were lysed in radioimmunoprecipitation assay (RIPA, Solarbio, Beijing, China) lysis buffer containing phenylmethane-sulfonyl fluoride (PMSF, 100:1; Solarbio) for 2 h, and then were centrifuged at 4°C, 16,000 g for 10 min. The total protein content in each sample was detected using a Pierce[™] Rapid Gold BCA (bicinchoninic acid) Protein Assay Kit (Thermo Scientific, Shanghai, China),¹⁹ and mixed with SDS sample buffer (1:1) and boiled for 10 min at 95°C. Samples (equivalent to 30 μ g total protein) were separated by 10–12% sodium dodecyl sulfate-polyacrylamide gel electrophoresis (SDS-PAGE) and transferred onto a polyvinylidene difluoride (PVDF) membrane. Membranes were blocked with 5% skimmed milk in 1 \times Tris-buffered saline (TBS) containing 0.1% Tween-20 for 2 h at room temperature, then incubated with the primary antibody in antibody dilution buffer (Beyotime, Shanghai, China) at 4°C overnight. Primary antibodies included anti-GSDMD (PA5-116,815, 1:1000, Invitrogen), anti-caspase-3 (D3R6Y, 1:1000, CST), anti-Bcl2 (2876S, 1:1000, CST), anti-Bax (2772S, 1:1000, CST) and anti-GAPDH (14C10, 1:1000, CST). The following day, membranes were washed with 1 \times Tris-buffered saline and Tween 20 (TBST) three times and incubated with secondary antibody (111-035-045, 1:1000, Jackson ImmunoResearch, USA) at room temperature for 1 h. Protein expression levels were tested with chemiluminescence (ThermoFisher Scientific, Waltham, MA, USA). The ratio of the gray value of the target band to GAPDH was representative of the relative protein expression.

Transwell Assay

Migration assays were performed using transwell chambers (8 μ m pore size; Corning, Beijing, China). After dispersing HCECs with 0.25% trypsin, the cells were centrifuged and resuspended with a serum-free medium. And, 3×10^4 cells were inoculated into each chamber before the complete medium was added to the 24-well plate. After 48 h incubation at 37°C, the unigrated cells were removed. The cells on the transwell membranes were fixed with 4% paraformaldehyde for 30 min and stained with 0.5% crystal violet solution. After being rinsed with tap water, the migrated cells were counted under an inverted microscope.

Lactic Dehydrogenase (LDH) Activity Assay

LDH activity was measured to evaluate plasma membrane permeability with an LDH assay kit (Jiancheng, Nanjing, Jiangsu, China). Cells were grown in a 96-well plate for various treatments, and then the supernatants were harvested at the proper time. Cell supernatant was transferred into another 96-well plate and incubated with LDH working reagent for 35 min according to the manufacturer's instructions. Then, the absorbance of the samples was measured at 450 nm with a microplate reader (Epoch, USA). The level of LDH release was counted as the percentage of the total amount, considered as the sum of the enzymatic activity present in the cellular lysate and that in the cell supernatant.

IL-1 β and IL-18 Determination

The concentrations of IL-1 β and IL-18 in cell culture supernatants were determined using the human Interleukin 1 β ELISA Kit (E-EL-H0149c, Elabscience) and Human Interleukin 18 ELISA Kit (E-EL-H0253c, Elabscience) according to the manufacturer's protocol. Briefly, particulates were removed by centrifugation for 10 min at 1000 \times g, 4°C. Then, 100 μ L of the working standard and sample were added to each well, and after incubating for 1.5 h at 37°C, the samples were incubated with a biotin-labeled antibody (100 μ L/well) for 1 h at 37°C. After three washes with wash buffer (350 μ L/well), HRP-avidin (100 μ L/well) was added, and the samples were incubated for 30 min at 37°C. After five washes, TMB substrate (90 μ L/well) was added to each well, and the samples were incubated for 20 min at 37°C in the dark. Subsequently, 50 μ L of stop solution was added per well, and the optical density was examined at 450 nm with a Power Wave Microplate Reader (Bio-TEK, USA).

Immunofluorescence Staining

HCECs were cultured on eight-chamber slides and fixed with 4% paraformaldehyde in PBS for 15 min, then permeabilized with 0.5% Triton X-100 for 15 min, and blocked with 10% goat serum for 1 h. Samples were stained by anti-GSDMD antibody (1:50, Invitrogen) in antibody dilution buffer (Beyotime, Shanghai, China) at 4 °C overnight. Secondary staining was performed with Alexa Fluor™ 488 goat anti-rabbit IgG (1:200, Invitrogen, USA) for 1 h at room temperature, and the nuclei were counterstained with DAPI for 7 min.

Caspase-1 Activity Assay

Caspase-1 activity in HCE cells was measured using a commercial Caspase-1 Activity Assay Kit (C1101, Beyotime, Shanghai, China) according to the manufacturer's instructions. This assay is performed on the basis of the ability of caspase-1 to change acetyl-Tyr-Val-Ala-Asp p-nitroaniline (Ac-YVAD-pNA) into the yellow formazan product pNA. After treatment, cells were harvested and lysed. Protein concentration was then determined using the Bradford protein assay reagent (Bio-Rad, CA, USA) according to the manufacturer's instructions. Absorbance was measured at 405 nm by spectrophotometer (BioTek, VT Lab, USA). Standard curves for the assay system were obtained from dilutions of the standards of pNA. Caspase-1 activity was then obtained by determining the amount of pNA according to the standard curve of pNA.

Flow Cytometry

Flow cytometry was used to evaluate the apoptosis of HCECs. Briefly, the cells were resuspended in 1 \times binding buffer and double-stained with the fluorescein isothiocyanate (FITC) Annexin V-propidium iodide (PI) kit (Vazyme, Nanjing, Jiangsu, China). Finally, the FlowJo10.6.2 system was used to measure the apoptosis rate of HCECs according to the manufacturer's protocol. The number of independent experiments was three.

Statistical Analysis

Data analysis was performed using SPSS 22.0 (Chicago, USA) and GraphPad Prism 8 (California, USA). All data were shown as mean \pm standard deviation (SD) based on at least three repeats. Significance between two groups was evaluated using the independent Student's *t*-test. One-way ANOVA with Bonferroni correction was used to compare the difference among more than two groups. The results were considered to be statistically significant at $P < 0.05$.

Results

Hyperosmolarity Induced GSDMD-Dependent Pyroptosis in HCECs

Pyroptosis is triggered in a classical GSDMD-dependent pattern.¹¹ The data suggested that the level of GSDMD distinctly increased under the hyperosmolarity intervention of 70–110 mM (Figure 1A). Moreover, N-GSDMD is required by inflammatory caspases for pyroptosis.²⁰ N-GSDMD expression was notably increased in HCECs treated with hyperosmolarity (90–120 mM) compared with those observed in the control cells (Figure 1B and D). The data demonstrated that the level of mRNA and protein in GSDMD and N-GSDMD did not significantly increase once the

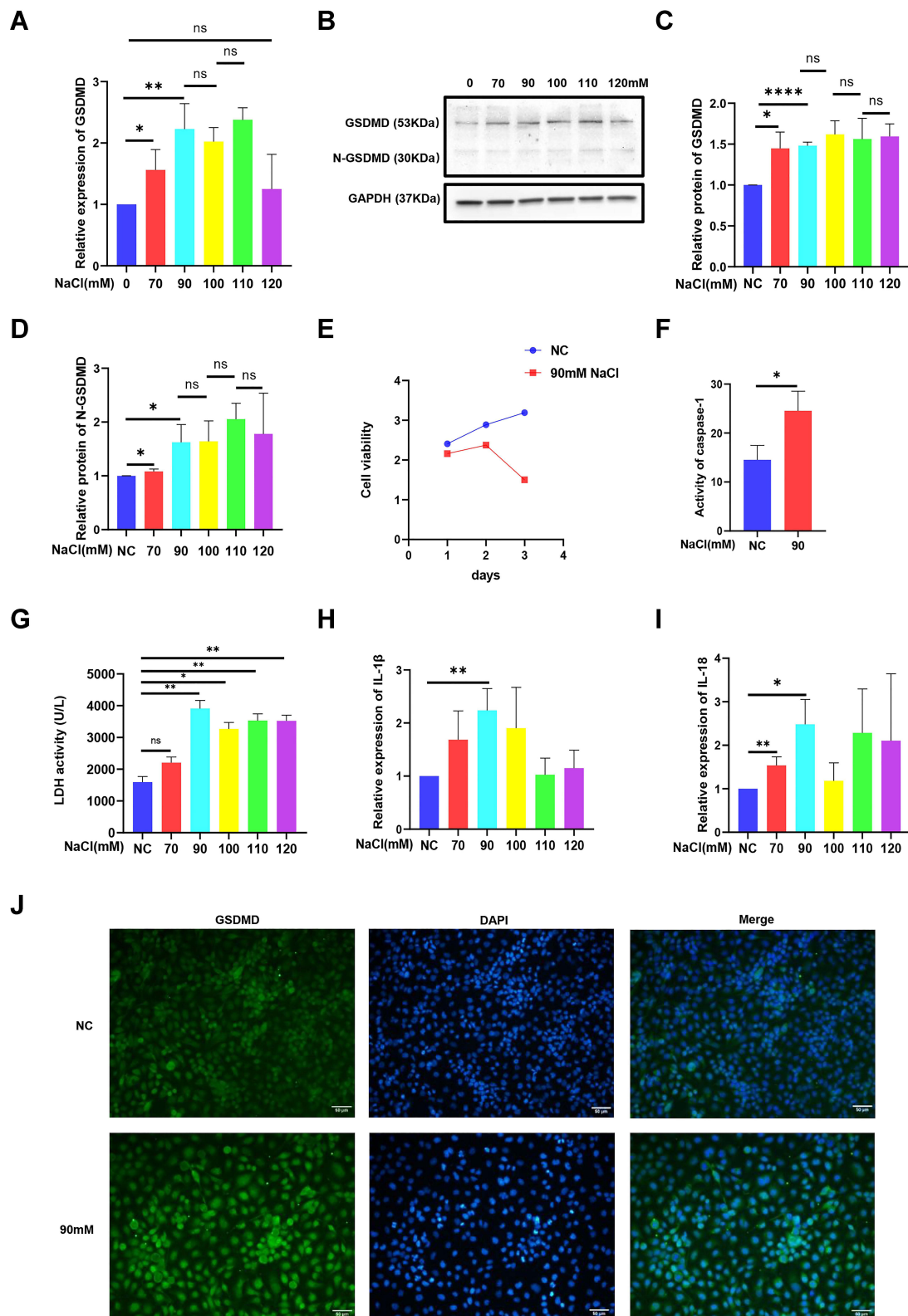


Figure 1 Hyperosmolarity induced GSDMD-dependent pyroptosis in HCECs. **(A)** The mRNA level of pyroptosis marker GSDMD was detected by RT-PCR. **(B–D)** The protein levels of pyroptosis markers (GSDMD and N-GSDMD) were detected by Western blotting. **(E)** Cell viability of HCECs treated with hyperosmolarity medium (90 mM) after 3 days. **(F)** The protein level of caspase-1 was detected by caspase-1 activity assay kit. **(G)** The release of lactate dehydrogenase (LDH) increased in hyperosmolarity stress (HS)-stimulated cells. **(H and I)** IL-1 β and IL-18 levels in the cell were detected by qRT-PCR. **(J)** Showing the distributions of GSDMD puncta in HCECs exposed to hyperosmotic medium (90 mM). Values are shown as mean \pm SD. *P<0.05, **P<0.01, ****P<0.0001.

medium osmolarity had risen between 100 and 120 mM (Figure 1A–D). Accordingly, 90mM was consistently used for the following experiments. Cell viability was estimated using the CCK-8 assay. The results showed that hyperosmolarity (90 mM) significantly decreased HCEC viability compared with that observed in the control group after 3 days (Figure 1E). Incubation of HCECs with hyperosmolarity (90 mM) led to notable increases in the caspase-1, LDH, IL-1 β , and IL-18 contents in culture supernatants (Figure 1F–I). In summary, hyperosmolarity could significantly promote an increased level of GSDMD, active cleavage of GSDMD, caspase-1, and the secretion of IL-1 β , IL-18, and LDH. Immunostaining demonstrated that GSDMD (green) fluorescence intensity was significantly increased in hyperosmolarity-treated compared with the control group (Figure 1J).

Hyperosmolarity Reduced the Migration of HCECs and Promoted Apoptosis

Normal HCECs are animated and present proliferation and migration abilities.²¹ Pyroptosis can decrease cell motility and proliferation.²² In our study, the mean number of migrated cells in the 70, 90, 100, 110, 120 mM hyperosmolarity-exposed HCECs was 4498, 3865, 3971, 3901, 2823 per well, respectively, which was obviously lower than the mean number of migrated control cells with 6065 per well (Figure 2A and B). Furthermore, cell migration is associated with apoptosis as well.²³ Therefore, we detected the expression of apoptosis marker caspase-3, Bcl-2, and Bax in HCECs exposed to the hyperosmotic medium for 24h. Apparently, the expression of caspase-3 increased (Figure 2C) while the ratio of Bcl-2/Bax decreased after being treated with the hyperosmolarity medium, which suggested that the hyperosmolarity promoted apoptosis (Figure 2D and E). Flow cytometry assays also showed that hyperosmolarity promoted the apoptosis of HCECs and early apoptotic cells were more dominant than late apoptotic cells, with percentages of 9.14% and 3.28% respectively (Figure 2F and G).

Hyperosmolarity Induced MIAT Upregulation and Knocking-Down MIAT Promoted Pyroptosis and Inhibited Proliferation in HCECs

In a previous study, it had been found that MIAT regulated primary human retinal pericyte pyroptosis in diabetic retinopathy.²⁴ In the present study, as shown in Figure 3A, treatment with different osmolarity (70, 90, 100, 110, 120 mM) from normal iso-osmolar medium (0 mM) MIAT expression in HCECs was significantly higher in the concentration of 90, 110 and 120 mM than that observed in the control group (Figure 3A). To explore the role of MIAT in pyroptosis, MIAT was knocked down in HCECs by siRNA. MIAT relative expression in the siMIAT group was 52% of the siNC control (Figure 3B). GSDMD, caspase-1 mRNA relative expression had a visible increase in the siMIAT group than in the siNC control group (Figure 3C and D). The protein level in cells increased as the mRNA level expression (Figure 3E–H). In addition, IL-1 β and IL-18 mRNA relative expression were detected to present a significant elevation in the siMIAT group than in the siNC control (Figure 3I and J). IL-1 β and IL-18 levels in cell supernatant were significantly increased in siMIAT than in the siNC (Figure 3K and L). The release of LDH in cell medium supernatant also increased (Figure 3M). These results verified that MIAT might negatively regulate caspase-1, GSDMD, IL-1 β , and IL-18 expression. It showed that MIAT seemed to inhibit pyroptosis in HCECs. The CCK-8 assay showed that siRNA-mediated knockdown of MIAT significantly decreased the viability of HCECs for 3 days (Figure 3N). The GSDMD (green) fluorescence observed in the hyperosmolarity group was also obviously detected after MIAT siRNA transfection (Figure 3O).

Knocking Down MIAT Inhibited the Migration and Promoted Apoptosis of HCECs

We then explored the role of MIAT in the mobility and growth of HCECs. The transwell assay showed that down-regulation of MIAT expression significantly inhibited the migration of HCECs (Figure 4A and B). The results of qRT-PCR indicated that the caspase-3 and caspase-8 increased and the ratio of Bcl-2/Bax decreased in the siMIAT group (Figure 4C–E). The protein expression of caspase-3 and caspase-8 also decreased after knocking down MIAT (Figure 4F and G). Flow cytometry assays showed that knockdown of MIAT by siRNA promoted the apoptosis of HCECs and late apoptotic cells were more dominant than early apoptotic cells, with percentages of 3.75% and 1.65%, respectively (Figure 4H and I).

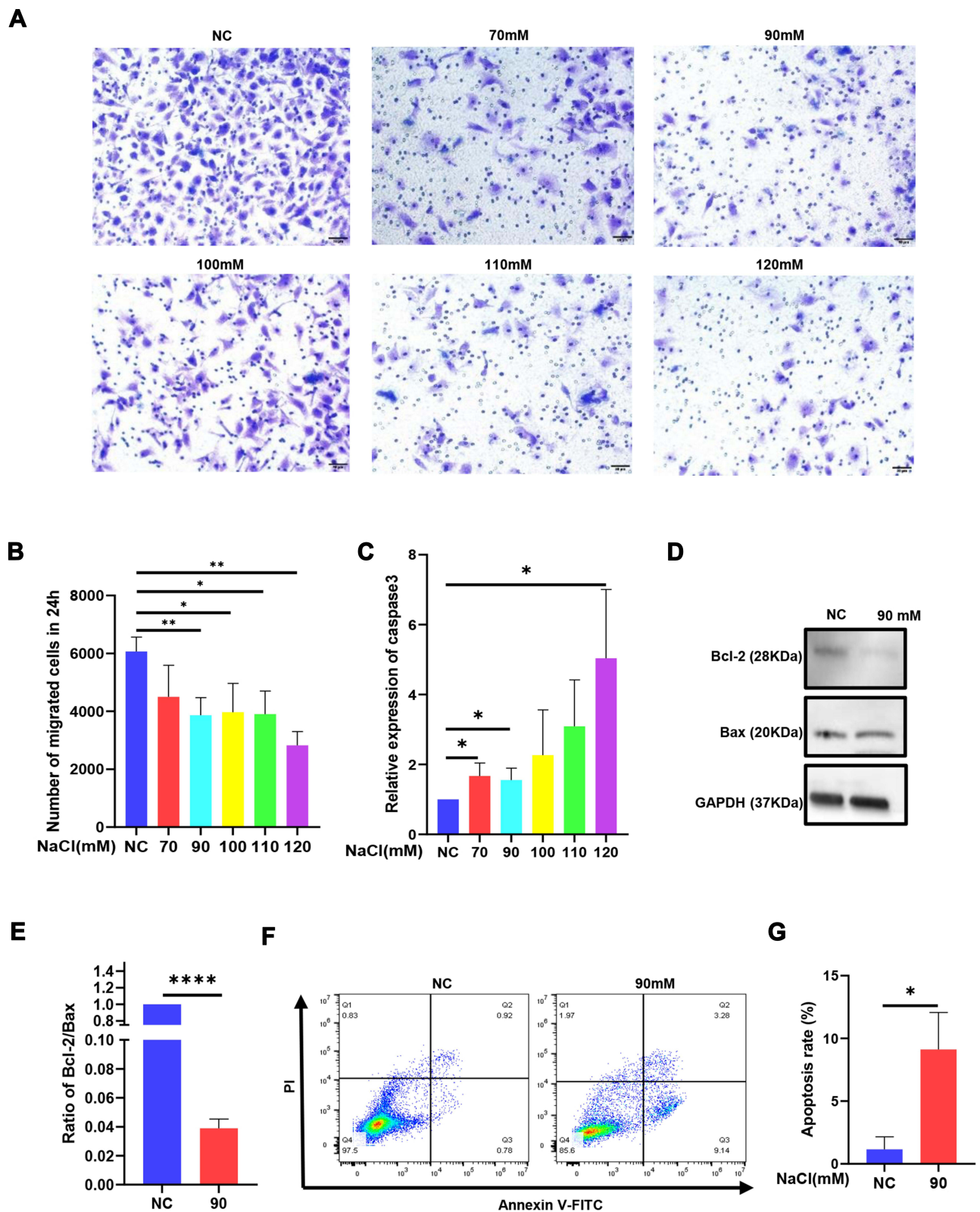


Figure 2 Hyperosmolarity reduced the migration of HCECs and promoted apoptosis. **(A and B)** Cell ability of migration was measured by transwell assay after HCECs treated with various concentrations of hyperosmolarity medium. The data are presented as the mean \pm SD, * p <0.05 compared with iso-osmotic as the control. **(C)** The mRNA level of apoptosis marker caspase-3 was detected by qRT-PCR. **(D and E)** The ratio of protein level of apoptosis marker (Bcl-2/Bax) was detected by Western blotting. **(F and G)** Cell apoptosis rate was evaluated in flow cytometry analysis. Data obtained from more than three repeated experiments were shown as mean \pm SD. * P <0.05, ** P <0.01, *** P <0.0001.

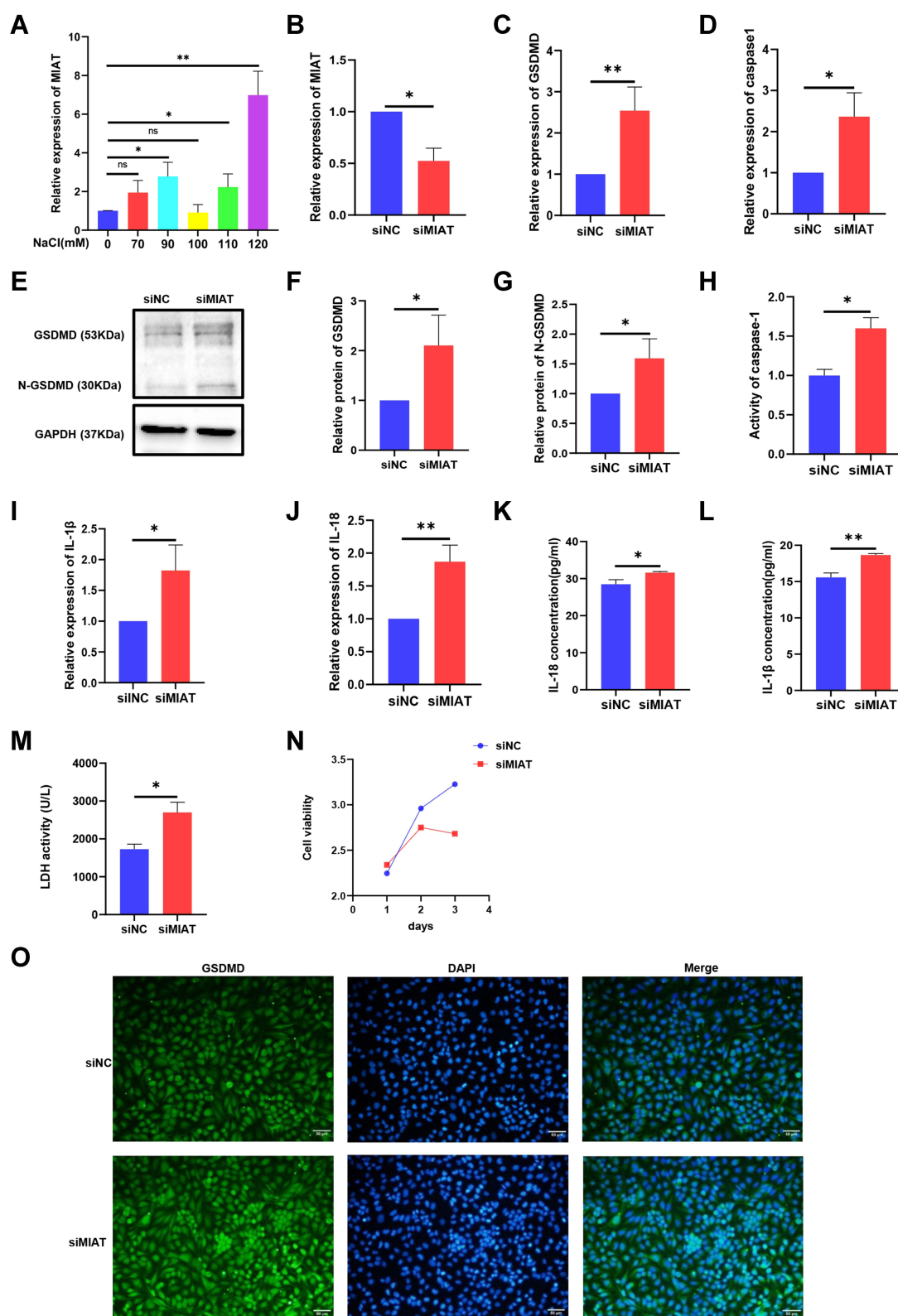


Figure 3 Hyperosmolarity induced MIAT upregulation and knocking-down MIAT promoted pyroptosis but inhibited proliferation in HCECs. **(A)** qRT-PCR assay revealed MIAT expression. **(B)** qRT-PCR assay revealed MIAT expression after being treated with transfected with MIAT-specific siRNA or a negative control siNC. **(C and D)** The mRNA levels of GSDMD and caspase-1 were detected by qRT-PCR versus the control group. **(E–H)** The protein levels of GSDMD and caspase-1 were detected by Western blotting and caspase-1 activity assay kit. **(I and J)** The mRNA levels of IL-1 β and IL-18 were detected by qRT-PCR. **(K and L)** The contents of IL-1 β and IL-18 in supernatants were examined by ELISA assay. **(M)** The release of lactate dehydrogenase (LDH) increased in siMIAT. **(N)** Cell viability of HCECs was decreased after knocking down MIAT in 3 days. **(O)** Showing the distributions of GSDMD puncta in HCECs after MIAT knockdown treatment. Data obtained from more than three repeated experiments were shown as mean \pm SD. *P < 0.05, **P < 0.01.

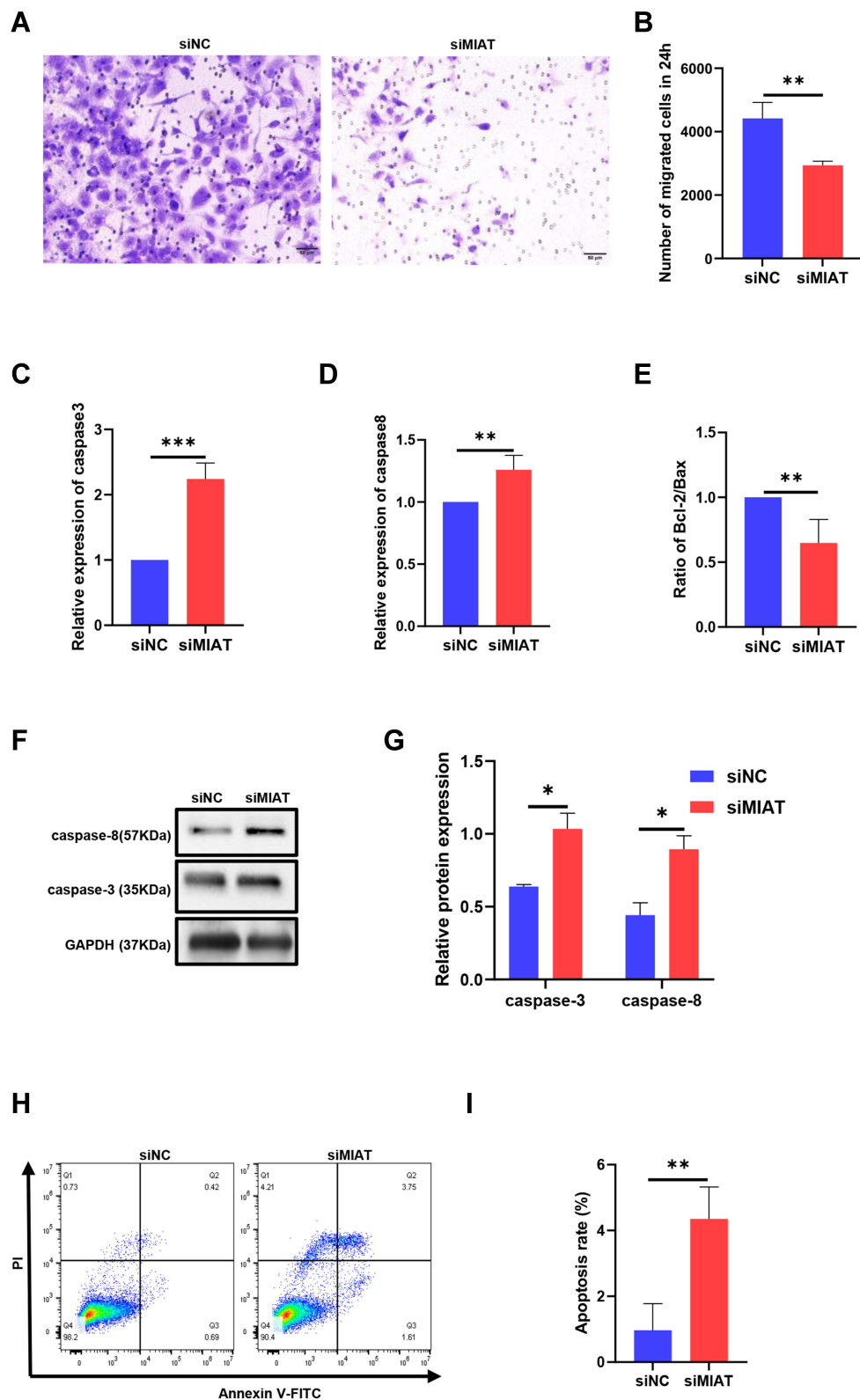


Figure 4 Knocking down MIAT inhibited the migration and promoted apoptosis of HCECs. (**A** and **B**) Cell ability of migration was measured by transwell assay after HCECs treated with transfection siRNA. (**C–E**) The mRNA levels of caspase-3, caspase-8, and the ratio of Bcl2/Bax were detected by qRT-PCR. ** $P < 0.01$, *** $P < 0.001$ compared with the control. (**F** and **G**) The protein levels of caspase-3 and caspase-8 were detected by Western blotting. * $P < 0.05$ compared with the control. (**H** and **I**) Cell apoptosis rate was evaluated in flow cytometry analysis. ** $P < 0.01$ compared with siNC as the control.

Caspase-1 Inhibitor Attenuates Pyroptosis Induced by HS and MIAT Knockdown

To investigate the potential mechanisms of pyroptosis in DED, we studied the role of the caspase-1 signaling pathway in the regulation of pyroptosis. We treated HCECs with the caspase-1 inhibitor Ac-YVAD-CHO for 24h and the concentration of 10 μ M led to a significant increase in cell viability (Figure 5A), thereby we used 10 μ M to perform the following tests. The results showed that N-GSDMD and caspase-1 expression as well as IL-1 β , IL-18 release from HCECs markedly reduced in the inhibitor group (Figure 5B), indicating that hyperosmolarity did induce the caspase-1-dependent pyroptosis of HCECs. Also, the caspase-1 inhibitor decreased the expression of GSDMD, IL-1 β , and IL-18 after MIAT siRNA transfection (Figure 5C). The protein level in cells decreased as the mRNA level expression (Figure 5D–I).

Caspase-1 Inhibitor Reversed Migration and Apoptosis in HCECs Induced by HS and MIAT Knockdown

In addition, the mean number of migrated cells in the 90 mM hyperosmolarity-exposed HCECs treated with Ac-YVAD-CHO was obviously higher than the mean number of migrated DMSO control cells (Figure 6A and B). Likewise, the inhibitor treatment significantly promoted the migration of HCECs in the siMIAT transfection group (Figure 6C and D). The proportion of apoptotic HS-stimulated cells decreased in Ac-YVAD-CHO, shown as the ratio of Bcl-2/Bax by Western blotting (Figure 6E and 6F). Flow cytometry assays showed that caspase-1 inhibitor reversed the apoptosis induced by HS (Figure 6G and H) and siMIAT (Figure 6I and J) treatment in HCECs. It showed that the caspase-1/GSDMD pyroptosis pathway seemed to mediate migration and apoptosis in HCECs.

Discussion

Increased tear osmolarity has been known as one of the core events in dry eye pathophysiology, inducing apoptosis of corneal and conjunctival cells and motivating inflammatory cascades that cause further cell death.²⁵ In our study, we established a dry eye model using HCECs, which demonstrated that hyperosmolarity promoted pyroptosis *in vitro* and confirmed the significantly enhanced expression of MIAT in the dry eye compared to the control. The results seemed to show that the increase of MIAT expression was relative to the pyroptosis in dry eye.

Hyperosmotic insult significantly activated inflammatory reactions and inflammation is always accompanied by cell death.²⁶ Cell death has physiological and pathological functions. Apoptosis, necroptosis, and pyroptosis are the three forms of programmed cell death with well-understood mechanisms. Apoptosis is an indispensable physiological process of tissue formation during embryogenesis and even after birth, and it results in the controlled death of the cell without releasing its contents out of the cells.²⁷ Differed from apoptosis, necroptosis and pyroptosis allow the release of immunogenic cellular content, including damage-associated molecular patterns (DAMPs), and inflammatory cytokines, which trigger inflammation.²⁸ Necroptosis is a mechanism of regulated necrotic death,²⁹ which is triggered when apoptosis is suppressed and it seems that caspase-8 inhibits necroptotic signaling.^{30,31} Pyroptosis has a lytic phenomenon characterized by cell swelling with large bubbles blowing out of the serosal membrane via destroying pathogen replication niche and intracellular traps induced by pores, and GSDMD and caspase-1 are required for the formation of plasma membrane pores.^{32,33} Unlike apoptosis, nuclear integrity is maintained in pyroptosis.³⁴ Chen et al showed increased N-GSDMD levels in the corneal epithelium of mice exposed to desiccating stress (DS) when compared to the controls.¹⁶

In the present study, we tend to examine the pyroptosis phenotype in our cell model. One of the findings of our work is that hyperosmolarity initiated GSDMD-dependent pyroptosis in HCECs shown as elevation of its executor N-GSDMD and the upregulation of caspase-1, as well as the increased release of proinflammatory cytokines IL-1 β , IL-18 and LDH. We noticed that the concentration of 90 mM induced the expression of both GSDMD and N-GSDMD and their expressions did not elevate markedly with higher concentrations. In our previous study, HMGB1 increased significantly in the same concentration as well in vivo and in vitro.¹⁸ HMGB1 secretion was dependent on the inflammasome components' apoptotic speck protein containing a caspase activation and recruitment domain (ASC) and caspase-1.³⁵

More recent data showed that caspase-8 promotes NLRP3 activation by cleaving GSDMD directly, thereby promoting pyroptosis downstream of TNF and providing protection against infection in vivo.^{36,37} Subsequently, we noticed upregulated expressions of caspase-3, caspase-8, and downregulated of Bcl-2/Bax, which means apoptosis was also

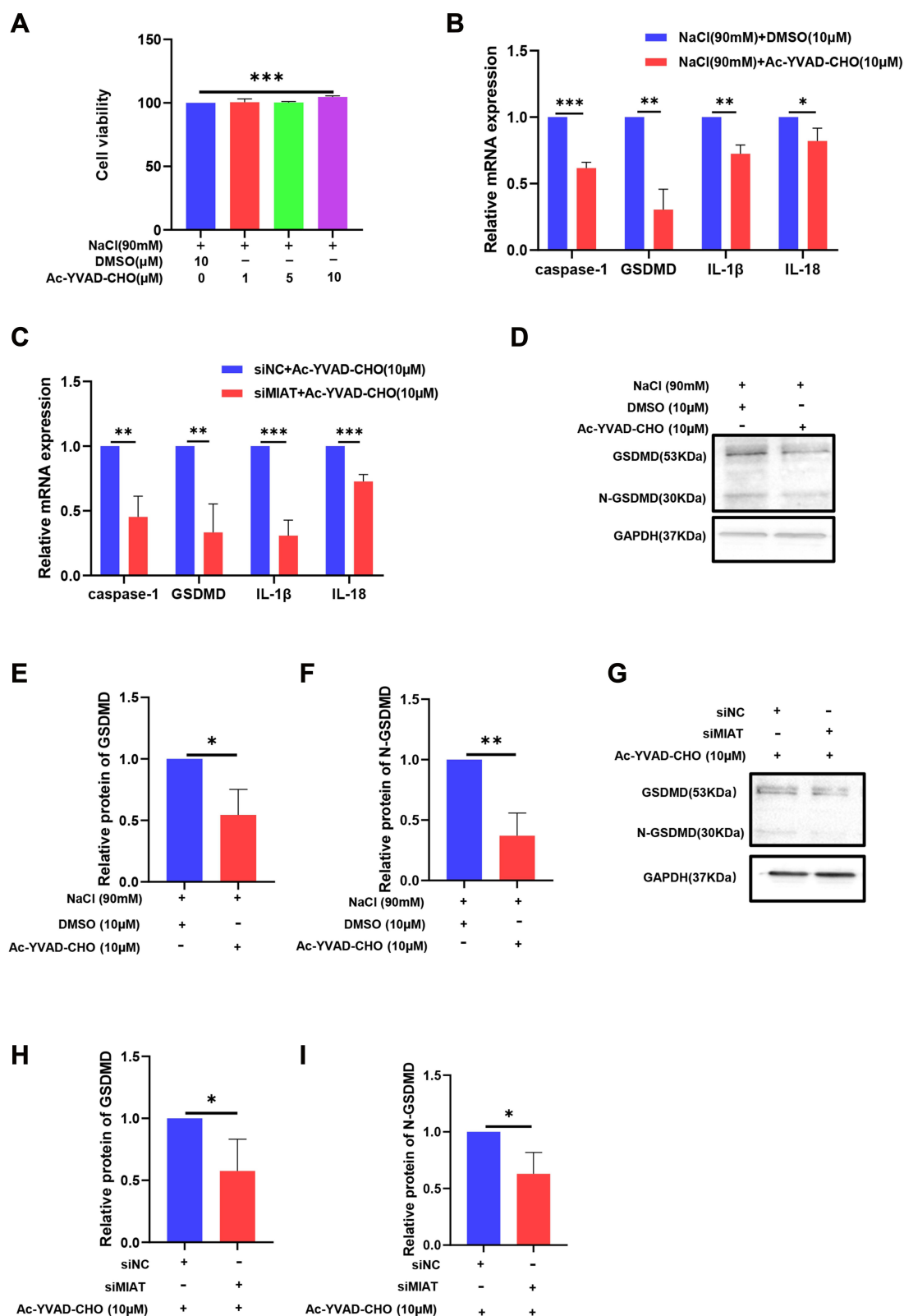


Figure 5 Caspase-1 inhibitor attenuates pyroptosis induced by hyperosmolarity stress (HS) and MIAT knockdown and regulates apoptosis in HCECs. **(A)** Cell viability of HCECs treated with various concentrations of Ac-YVAD-CHO (1, 5, 10 μ M). **(B)** Ac-YVAD-CHO treatment (10 μ M) suppressed caspase-1, GSDMD, IL-1 β , and IL-18 in mRNA levels in HS-stimulated cells. **(C)** Ac-YVAD-CHO treatment (10 μ M) suppressed caspase-1, GSDMD, IL-1 β , and IL-18 in mRNA level in siRNA cells. **(D–I)** Ac-YVAD-CHO treatment (10 μ M) suppressed GSDMD and N-GSDMD in protein level in both HS-stimulated cells and siMIAT cells, values are shown as mean \pm SD. *P<0.05, **P<0.01, ***P<0.001.

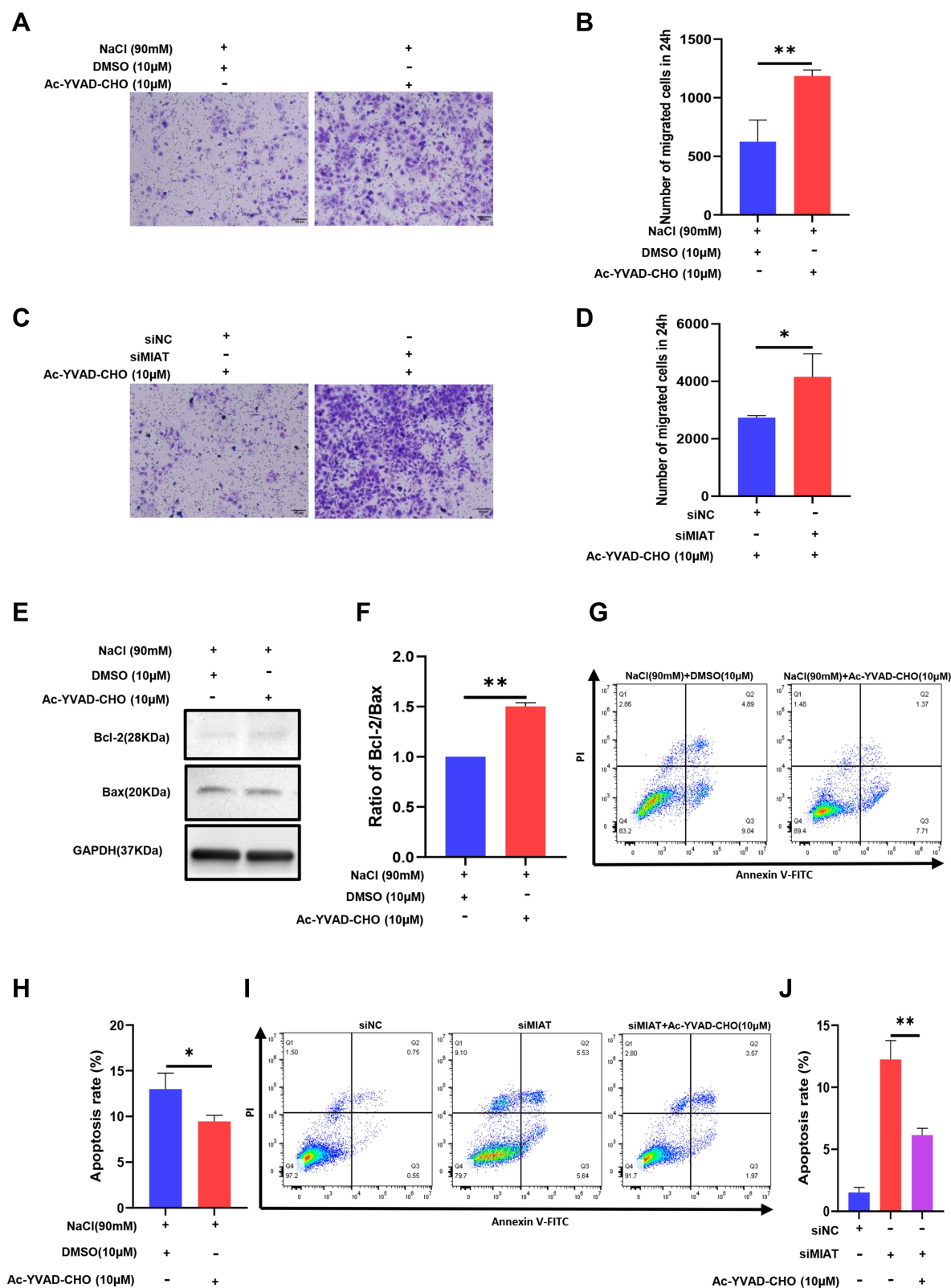


Figure 6 Caspase-1 inhibitor reversed migration and apoptosis in HCECs induced by hyperosmolarity stress (HS) and MIAT knockdown. **(A and B)** Cell ability of migration was measured by transwell assay after HCECs were treated with 90mM concentrations of hyperosmolarity medium and Ac-YVAD-CHO treatment (10 μM). **(C and D)** Cell ability of migration was measured by transwell assay treated with transfection siRNA and Ac-YVAD-CHO treatment (10 μM). **(E and F)** Ac-YVAD-CHO treatment (10 μM) reduced the proportion of apoptotic HS-stimulated cells, shown as ratio of Bcl-2/Bax by Western blotting. **(G and H)** Cell apoptosis rate decreased in flow cytometry analysis after Ac-YVAD-CHO treatment (10 μM) in the DE group. **(I and J)** Cell apoptosis rate decreased in flow cytometry analysis after Ac-YVAD-CHO treatment (10 μM) in knockdown MIAT group. The ratio of values are shown as mean ± SD. *P<0.05, **P<0.01.

promoted by hyperosmolarity stress. These results were also verified by flow cytometry. When pyroptosis occurs, the migration and proliferation ability of cells are weakened.²² To clarify the effect of HS on migration and proliferation of HCECs, we performed transwell assay and CCK8 experiments and detected that the ability of migration and proliferation of cells was reduced expectedly. We speculated that pyroptosis and apoptosis occurred simultaneously when hyperosmolarity stress appears in dry eye disease, and the migration of the cells was inhibited.

Caspase-1 has the potential to induce pyroptosis and apoptosis in a manner that is dependent on the expression of the pyroptosis mediator gasdermin D.³⁸ Exogenous supplementation of a reported caspase-1 inhibitor, Ac-YVAD-CHO,³⁹ could reduce the expression of pyroptosis and apoptosis markers in HCEC, further confirming the contribution of pyroptosis and apoptosis toward caspase-1 processes. At the concentration of 10 μ M, the migration and proliferation of HCECs were markedly increased compared to DMSO control after hyperosmolarity treatment.

It had been revealed that MIAT was involved in the pathological angiogenesis of diabetes and affected the proliferation, apoptosis, and migration of human lens epithelial cells (HLEC) upon oxidative stress in posterior capsule opacification.^{9,40,41} However, the relationship between MIAT and hyperosmolarity stress in HCECs has not been reported. In this study, we confirmed the upregulation of MIAT in HS-induced HCECs and we explored the role of MIAT in HCECs by knocking down MIAT using siRNA. We found that knockdown MIAT significantly facilitated the pyroptosis phenotype, including the upregulation of caspase-1 and GSDMD. Our data also showed that pro-inflammatory cytokines IL-1 β , IL-18, and LDH increased release with MIAT knockdown. Therefore, we investigated that MIAT has a potential effect of inhibiting caspase-1 and GSDMD expression and consequent HCEC pyroptosis, whereas Yu et al showed that MIAT promoted pericyte pyroptosis in diabetic retinopathy.²⁴ The discrepancy in our conclusions may result from the differences in cells and stimulation conditions. These results indicated that MIAT may play an essential role in the hyperosmolarity-induced pyroptosis of HCECs. The impact of MIAT silencing on the reduction of cell viability, proliferation, and invasion, while enhancement of cellular senescence and apoptosis has been reported.⁴² This is consistent with our results showing that the migration and proliferation of HCECs with suppressed MIAT expression were lower than those in the negative control, while the apoptosis rate elevated higher. These results suggested that the migration ability of cells was weakened when apoptosis happened. Our experimental results implied that MIAT can inhibit pyroptosis and apoptosis in HCECs while mediating the ability of migration of HCECs positively. We speculated that, on the one hand, the upregulated MIAT resisted pyroptosis and apoptosis, which were stimulated by increased tear osmolarity, on the other hand, MIAT promoted migration to protect HCEC from injury in dry eye. The effect of MIAT in this study is similar to that found by Shen et al who documented that MIAT knockdown significantly decreased the HLEC viability and proliferative ability, and mediated HLEC apoptosis.⁴¹ However, Zhang et al suggested that MIAT could promote high glucose-induced Müller cell apoptosis.^{24,43} We hypothesized that MIAT displayed different effects in different ocular cells due to the existence of a blood-retinal barrier and no vascular in the cornea or lens because MIAT is an important regulator of vascular remodeling.⁹

Caspase-1 inhibitor, Ac-YVAD-CHO, partially reversed the effects of siMIAT on HCEC apoptosis and migration, further confirming the contribution of pyroptosis toward caspase-1 processes. Therefore, we concluded that MIAT regulated pyroptosis, apoptosis, and migration mediated by caspase-1 in HS-induced inflammation in HCECs.

Conclusion

Our study adds to the accumulating evidence that MIAT is a critical mediator in the pyroptosis and apoptosis of HCECs dry eye model induced by hyperosmolarity stress. Functionally, we discover that MIAT regulates GSDMD-dependent-pyroptosis, apoptosis, and the downstream processes of cell viability and migration mediated by caspase-1, which indicates that MIAT might play a role in the pathogenesis of dry eye and act as a novel and potential factor for finding out the therapeutic targets in dry eye.

Acknowledgments

The authors were sponsored by the Natural Science Foundation of Shandong (ZR2019MH115), the National Natural Science Foundation of China (81201060) and the Clinical Medicine +X Research Project of The Affiliated Hospital of

Qingdao University (QDFY+X202101044). The sponsors or funding organizations had no role in the design or conduct of this research.

Disclosure

The authors report no conflicts of interest in this work.

References

- Craig JP, Nichols KK, Akpek EK, et al. TFOS DEWS II definition and classification report. *Ocul Surf*. 2017;15(3):276–283. doi:10.1016/j.jtos.2017.05.008
- Pflugfelder SC, de Paiva CS. The pathophysiology of dry eye disease: what we know and future directions for research. *Ophthalmology*. 2017;124(11s):S4–S13. doi:10.1016/j.ophtha.2017.07.010
- Yamaguchi T. Inflammatory Response in Dry Eye. *Invest Ophthalmol Vis Sci*. 2018;59(14):Des192–Des199. doi:10.1167/iov.17-23651
- Bucolo C, Fidilio A, Fresta CG, et al. Ocular pharmacological profile of hydrocortisone in dry eye disease. *Front Pharmacol*. 2019;10:1240. doi:10.3389/fphar.2019.01240
- Yang Y, Chen M, Zhai Z, et al. Long non-coding RNAs Gabarapl2 and Chrnb2 positively regulate inflammatory signaling in a mouse model of dry eye. *Front Med*. 2021;8:808940. doi:10.3389/fmed.2021.808940
- Yu Q, Guo W, Shen J, Lv Y. Effect of glucocorticoids on lncRNA and mRNA expression profiles of the bone microcirculatory endothelial cells from femur head of Homo sapiens. *Genom Data*. 2015;4:140–142. doi:10.1016/j.gdata.2015.04.013
- Rinn JL, Chang HY. Genome regulation by long noncoding RNAs. *Annu Rev Biochem*. 2012;81(1):145–166. doi:10.1146/annurev-biochem-051410-092902
- Zhang L, Dong Y, Wang Y, et al. Long non-coding RNAs in ocular diseases: new and potential therapeutic targets. *FEBS J*. 2019;286(12):2261–2272. doi:10.1111/febs.14827
- Jiang Q, Shan K, Qun-Wang X, et al. Long non-coding RNA-MIAT promotes neurovascular remodeling in the eye and brain. *Oncotarget*. 2016;7(31):49688–49698. doi:10.18632/oncotarget.10434
- Wang Z, Kun Y, Lei Z, Dawei W, Lin P, Jibo W. LncRNA MIAT downregulates IL-1 β , TNF- α to suppress macrophage inflammation but is suppressed by ATP-induced NLRP3 inflammasome activation. *Cell Cycle*. 2021;20(2):194–203. doi:10.1080/15384101.2020.1867788
- Shi J, Gao W, Shao F. Pyroptosis: gasdermin-mediated programmed necrotic cell death. *Trends Biochem Sci*. 2017;42(4):245–254. doi:10.1016/j.tibs.2016.10.004
- He WT, Wan H, Hu L, et al. Gasdermin D is an executor of pyroptosis and required for interleukin-1 β secretion. *Cell Res*. 2015;25(12):1285–1298. doi:10.1038/cr.2015.139
- Homme RP, Singh M, Majumder A, et al. Remodeling of retinal architecture in diabetic retinopathy: disruption of ocular physiology and visual functions by inflammatory gene products and pyroptosis. *Front Physiol*. 2018;9:1268. doi:10.3389/fphys.2018.01268
- Chen H, Deng Y, Gan X, et al. NLRP12 collaborates with NLRP3 and NLRC4 to promote pyroptosis inducing ganglion cell death of acute glaucoma. *Mol Neurodegener*. 2020;15(1):26. doi:10.1186/s13024-020-00372-w
- Zhao W, Yang H, Lyu L, et al. GSDMD, an executor of pyroptosis, is involved in IL-1 β secretion in *Aspergillus fumigatus* keratitis. *Exp Eye Res*. 2021;202:108375. doi:10.1016/j.exer.2020.108375
- Chen H, Gan X, Li Y, et al. NLRP12- and NLRC4-mediated corneal epithelial pyroptosis is driven by GSDMD cleavage accompanied by IL-33 processing in dry eye. *Ocul Surf*. 2020;18(4):783–794. doi:10.1016/j.jtos.2020.07.001
- Zhang WH, Wang X, Narayanan M, et al. Fundamental role of the Rip2/caspase-1 pathway in hypoxia and ischemia-induced neuronal cell death. *Proc Natl Acad Sci U S A*. 2003;100(26):16012–16017. doi:10.1073/pnas.2534856100
- Li H, Li J, Hou C, Li J, Peng H, Wang Q. The effect of astaxanthin on inflammation in hyperosmolarity of experimental dry eye model in vitro and in vivo. *Exp Eye Res*. 2020;197:108113. doi:10.1016/j.exer.2020.108113
- Xue M, Liang H, Zhou Z, et al. Effect of fucoidan on ethanol-induced liver injury and steatosis in mice and the underlying mechanism. *Food Nutr Res*. 2021;2021:65.
- Karmakar M, Minns M, Greenberg EN, et al. N-GSDMD trafficking to neutrophil organelles facilitates IL-1 β release independently of plasma membrane pores and pyroptosis. *Nat Commun*. 2020;11(1):2212. doi:10.1038/s41467-020-16043-9
- Ljubimov AV, Saghizadeh M. Progress in corneal wound healing. *Prog Retin Eye Res*. 2015;49:17–45. doi:10.1016/j.preteyeres.2015.07.002
- Jiang C, Jiang L, Li Q, et al. Acrolein induces NLRP3 inflammasome-mediated pyroptosis and suppresses migration via ROS-dependent autophagy in vascular endothelial cells. *Toxicology*. 2018;410:26–40. doi:10.1016/j.tox.2018.09.002
- Sun Y, Liu WZ, Liu T, Feng X, Yang N, Zhou HF. Signaling pathway of MAPK/ERK in cell proliferation, differentiation, migration, senescence and apoptosis. *J Recept Signal Transduct Res*. 2015;35(6):600–604. doi:10.3109/10799893.2015.1030412
- Yu X, Ma X, Lin W, Xu Q, Zhou H, Kuang H. Long noncoding RNA MIAT regulates primary human retinal pericyte pyroptosis by modulating miR-342-3p targeting of CASP1 in diabetic retinopathy. *Exp Eye Res*. 2021;202:108300. doi:10.1016/j.exer.2020.108300
- Luo L, Li DQ, Corrales RM, Pflugfelder SC. Hyperosmolar saline is a proinflammatory stress on the mouse ocular surface. *Eye Contact Lens*. 2005;31(5):186–193. doi:10.1097/01.ICL.0000162759.79740.46
- Van Oudenbosch N, Lamkanfi M. Caspases in cell death, inflammation, and disease. *Immunity*. 2019;50(6):1352–1364. doi:10.1016/j.immuni.2019.05.020
- Kaiser WJ, Daley-Bauer LP, Thapa RJ, et al. RIP1 suppresses innate immune necrotic as well as apoptotic cell death during mammalian parturition. *Proc Natl Acad Sci U S A*. 2014;111(21):7753–7758. doi:10.1073/pnas.1401857111
- Frank D, Vince JE. Pyroptosis versus necroptosis: similarities, differences, and crosstalk. *Cell Death Differ*. 2019;26(1):99–114. doi:10.1038/s41418-018-0212-6
- Li J, McQuade T, Siemer AB, et al. The RIP1/RIP3 necrosome forms a functional amyloid signaling complex required for programmed necrosis. *Cell*. 2012;150(2):339–350. doi:10.1016/j.cell.2012.06.019

30. Brault M, Oberst A. Controlled detonation: evolution of necroptosis in pathogen defense. *Immunol Cell Biol.* 2017;95(2):131–136. doi:10.1038/icb.2016.117
31. Oberst A, Dillon CP, Weinlich R, et al. Catalytic activity of the caspase-8-FLIP (L) complex inhibits RIPK3-dependent necrosis. *Nature.* 2011;471(7338):363–367. doi:10.1038/nature09852
32. Jorgensen I, Miao EA. Pyroptotic cell death defends against intracellular pathogens. *Immunol Rev.* 2015;265(1):130–142. doi:10.1111/imr.12287
33. Miao EA, Leaf IA, Treuting PM, et al. Caspase-1-induced pyroptosis is an innate immune effector mechanism against intracellular bacteria. *Nat Immunol.* 2010;11(12):1136–1142. doi:10.1038/ni.1960
34. Hersh D, Monack DM, Smith MR, Ghori N, Falkow S, Zychlinsky A. The salmonella invasin SipB induces macrophage apoptosis by binding to caspase-1. *Proc Natl Acad Sci U S A.* 1999;96(5):2396–2401. doi:10.1073/pnas.96.5.2396
35. Lamkanfi M, Sarkar A, Vande Walle L, et al. Inflammasome-dependent release of the alarmin HMGB1 in endotoxemia. *J Immunol.* 2010;185(7):4385–4392. doi:10.4049/jimmunol.1000803
36. Sarhan J, Liu BC, Muendlein HI, et al. Caspase-8 induces cleavage of gasdermin D to elicit pyroptosis during Yersinia infection. *Proc Natl Acad Sci U S A.* 2018;115(46):E10888–E10897. doi:10.1073/pnas.1809548115
37. Bertheloot D, Latz E, Franklin BS. Necroptosis, pyroptosis and apoptosis: an intricate game of cell death. *Cell Mol Immunol.* 2021;18(5):1106–1121.
38. Tsuchiya K. Inflammasome-associated cell death: pyroptosis, apoptosis, and physiological implications. *Microbiol Immunol.* 2020;64(4):252–269. doi:10.1111/1348-0421.12771
39. Wang J, Wang L, Zhang X, et al. Cathepsin B aggravates acute pancreatitis by activating the NLRP3 inflammasome and promoting the caspase-1-induced pyroptosis. *Int Immunopharmacol.* 2021;94:107496. doi:10.1016/j.intimp.2021.107496
40. Yan B, Yao J, Liu JY, et al. lncRNA-MIAT regulates microvascular dysfunction by functioning as a competing endogenous RNA. *Circ Res.* 2015;116(7):1143–1156. doi:10.1161/CIRCRESAHA.116.305510
41. Shen Y, Dong LF, Zhou RM, et al. Role of long non-coding RNA MIAT in proliferation, apoptosis and migration of lens epithelial cells: a clinical and in vitro study. *J Cell Mol Med.* 2016;20(3):537–548. doi:10.1111/jcmm.12755
42. Ghafouri-Fard S, Azimi T, Taheri M. Myocardial Infarction Associated Transcript (MIAT): review of its impact in the tumorigenesis. *Biomed Pharmacother.* 2021;133:111040. doi:10.1016/j.biopha.2020.111040
43. Zhang J, Chen M, Chen J, et al. Long non-coding RNA MIAT acts as a biomarker in diabetic retinopathy by absorbing miR-29b and regulating cell apoptosis. *Biosci Rep.* 2017;37(2):BSR20170036.

Publish your work in this journal

The Journal of Inflammation Research is an international, peer-reviewed open-access journal that welcomes laboratory and clinical findings on the molecular basis, cell biology and pharmacology of inflammation including original research, reviews, symposium reports, hypothesis formation and commentaries on: acute/chronic inflammation; mediators of inflammation; cellular processes; molecular mechanisms; pharmacology and novel anti-inflammatory drugs; clinical conditions involving inflammation. The manuscript management system is completely online and includes a very quick and fair peer-review system. Visit <http://www.dovepress.com/testimonials.php> to read real quotes from published authors.

Submit your manuscript here: <https://www.dovepress.com/journal-of-inflammation-research-journal>